PERGAMON

Vision Research 41 (2001) 173–186

Vision Research

www.elsevier.com/locate/visres

Visual jitter: evidence for visual-motion-based compensation of retinal slip due to small eye movements

Ikuya Murakami [a,*], Patrick Cavanagh [b]

[a] *Human and Information Science Laboratory, NTT Communication Science Laboratories, 3-1 Morinosato Wakamiya, Atsugi, Kanagawa 243-0198, Japan*

[b] *Department of Psychology, Harvard University, 33 Kirkland Street, Cambridge, MA 02138, USA*

Received 21 January 2000; received in revised form 4 August 2000

Abstract

When dynamic random noise is replaced by static noise after a period of adaptation, adjacent unadapted regions filled with static noise appear to 'jitter' coherently in random directions for several seconds, actually mirroring the observer's own eye movements of fixation [Murakami, I. & Cavanagh, P. (1998). *Nature*, *395*, 798–801]. The present study aims at psychophysically locating two distinct stages underlying this visual jitter phenomenon: a monocular, adaptable stage that measures local retinal motion and a compensation stage that estimates a baseline motion minimum and subtracts it from motion vectors nearby. The first three experiments revealed that visual jitter has storage, directional selectivity, and spatial frequency selectivity, like the motion aftereffect does. These results suggest some overlap in the adaptation mechanisms for the two effects, possibly at or below the level of primary visual cortex. The next two experiments revealed the transfer of the effect across the vertical meridian as well as the existence of a preferred stimulus size that is a linear increasing function of eccentricity, mimicking the RF size of the monkey MT neurons. These results suggest that some extrastriate motion area along the parietal pathway including MT mediates motion-based compensation of retinal slip.

Keywords: Visual jitter; Retinal slip; Adaptation; Compensation; Small eye movements

1. Introduction

Retinal image motion contains components generated by movements of external objects and by movements of the observer's head. These components are useful in recovering object motion as well as self-motion (Riggs, Armington, & Ratliff, 1954; Ditchburn & Foley-Fisher, 1967; Steinman, Haddad, Skavenski, & Wyman, 1973). However, the movements of the eye relative to the orbit also generates retinal image motion. These are undesirable image perturbations caused by the lack of stability of the input device and they need to be corrected — especially when they are from the small, incessant eye movements that occur during fixation. By analogy, watching a movie made with a hand-held camcorder can be annoying or even nauseating unless the camera has built in image-stabilizing algorithms (Patti, Tekalp, & Sezan, 1998).

Fixational eye movements are a mixture of slow drift, rapid microsaccades, and high-frequency tremor (Riggs et al., 1954; Ditchburn & Foley-Fisher, 1967; Steinman et al., 1973). On the one hand, these incessant movements have functional significance of their own, for if the visual image were completely stabilized on the retina, it would quickly fade (Riggs, Ratliff, Cornsweet, & Cornsweet, 1953; Yarbus, 1967). On the other hand, they bring about the challenging task of reconstructing a stable visual world from such jittery retinal inputs.

Theoretically, there are three major sources of biological signals for the compensation. The first one is 'corollary discharge' or efference copy of the motor commands that drive eye muscles (Helmholtz, 1866). The second one is proprioceptive feedback from eye muscles (Helmholtz, 1866). The third one is retinal image motion itself. The first and second, which have been termed 'outflow theory' and 'inflow theory', re-

* Corresponding author. Tel.: +81-46-2403596; fax: +81-46-2404716.

E-mail address: ikuya@apollo3.brl.ntt.co.jp (I. Murakami).

0042-6989/01/$ - see front matter
PII: S0042-6989(00)00237-6

spectively, both rely on extraretinal signals that can properly register instantaneous eye positions or velocities. In reality, however, the gain of extraretinal signals is reported to be far less than unity (e.g. Grüsser, Krizič, & Weiss, 1987; Wertheim, 1987; Freeman & Banks, 1998; Freeman, 1999), and there is no reason to assume that the situation is any better for small eye movements. Also, calibration based on extraretinal signals may be too slow to catch up with rapid, small eye movements (Grüsser et al., 1987). Furthermore, the eye's tiny motion relative to the world may have other origins not captured by efference copy or proprioceptive feedback: head movements (which always occur while speaking, chewing, and even standing as still as possible) result in mechanical vibrations of the eyes that cannot be fully stabilized by the vestibulo-ocular reflex (Skavenski, Hansen, Steinman, & Winterson, 1979). Therefore, compensating retinal slip using retinal image motion may be the only practical strategy for canceling small eye movements.

A new illusion that strongly supports this possibility has been previously reported (Murakami & Cavanagh, 1998). After adaptation to a patch of dynamic random noise (DRN), a larger pattern of static random noise (SRN) is presented. The SRN in the *unadapted* region then appears to 'jitter' coherently in random directions (see Fig. 1). It has been demonstrated that this jittery motion actually reflects the retinal slip due to the observer's small eye movements during fixation.[1] First, when there were many unadapted regions at remote locations, the jittering motions perceived in these separate regions were apparently synchronized, suggesting a single source of these illusory motions. Second, jitter was eliminated when the test stimulus was a stabilized retinal image. Third, when the experimenter artificially generated tiny eye movements of the subject (by post-

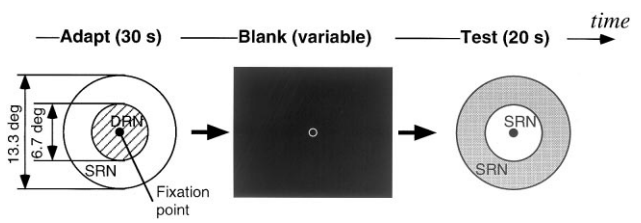

Fig. 1. A schematic of the storage experiment. The figures from left to right illustrate the time sequence: the adapting stimulus was presented for 30 s, then the whole display turned to black and stayed for a variable interval, and then the test stimulus was presented for 20 s. The hatched region indicates the adapted region, where dynamic random noise (DRN) was presented during the adaptation period. The shaded region indicates where visual jitter occurred in the test period. The ● indicates the location of the fixation point.

[1] The subject's eye movements have been recorded and it has been verified that the small eye movements are unchanged by our adapting stimuli.

rotational-nystagmus paradigm as well as by external force by a mechanical vibrator), the directions and frequency of visual jitter were as expected from the experimental manipulation of eye movements.

How does this jitter occur? It was proposed that retinal slip due to small eye movements is compensated solely on the basis of visual motion signals themselves. Without adaptation, retinal slip is fully represented in early visual cortex (Galletti, Squatrito, Battaglini, & Maioli, 1984; Gur & Snodderly, 1987, 1997; Ilg & Thier, 1996; Gur, Beylin, & Snodderly, 1997; Leopold & Logothetis, 1998). It was assumed that in this early stage, each retinotopic point has a motion vector (direction and speed) that is a mixture of eye movements and object motion. One of the missions of a processing stage higher than this early representation is to suppress the component of eye movements from this velocity field. It was proposed that a baseline value (i.e. eye velocity) is estimated by taking the velocity of the region having the minimum instantaneous velocity. This minimum velocity will usually, although not always, arise in regions of the scene where there is no external motion and so will represent eye movement velocity alone. By subtracting this baseline estimate from the velocities of all points, the desired zero velocity for the stationary regions and the correct velocity for the moving objects are recovered.

After adaptation to DRN, however, retinal slip is not encoded veridically: adaptation transiently attenuates responses to motion within the adapted region, creating a new baseline minimum velocity there. In the unadapted region, the unattenuated motion response to eye movements is now above the new, lower baseline. Therefore, the retinal slip is undercompensated and the residual is interpreted as a jittering motion in the *unadapted* region. In comparison, compensation based on any extraretinal signals should wrongly predict overcompensation and visual jitter in the *adapted* region (Murakami & Cavanagh, 1998).

This account of the visual jitter phenomenon postulates two distinct stages: an adaptable stage that measures local retinal motion, and a compensation stage that estimates a baseline motion minimum and subtracts it from motion vectors nearby. The present study aims at psychophysically locating each of these stages in the visual system.

2. Methods

The experiment was done in a semi-dark experimental booth. The stimulus was presented on a 20-inch color CRT monitor (SONY GDM2000TC, 832×624 pixels, vertical scanning frequency 75 Hz, non-interlaced) controlled by an Apple Power Macintosh computer. The subject's head motion was restricted with a

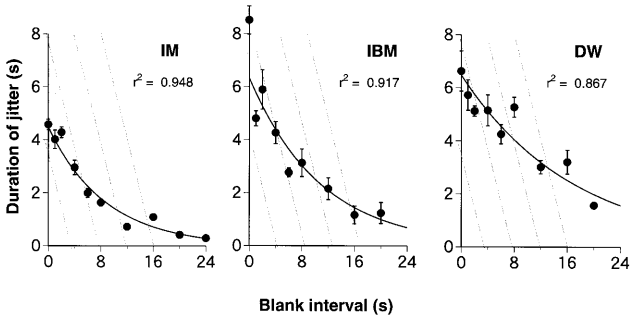

Fig. 2. The storage of visual jitter. The total duration of visual jitter (each point with an error bar indicates the mean ± 1 standard error (S.E.) of four repeated measurements) is plotted against the blank interval between adaptation and test. Each panel corresponds to each subject (the first author and two naive subjects participated; all had corrected-to-normal vision). The gray oblique lines indicate the constraint lines according to the null hypothesis of no storage: (duration of jitter) + (blank interval) = constant. The curved lines are the best-fit exponential functions.

chin rest and the viewing distance was 77.3 cm. Viewing was binocular.

A trial consisted of an adaptation period and a following test period. A fixation point was provided at the center of the monitor throughout the trial. The stimulus in the adaptation period had two regions, an 'adapted' region and an 'unadapted' region. In the adapted region, black and white DRN was presented; 50% of dots (each dot: 8 min × 8 min) were black (0.18 cd/m^2) and the remaining ones were white (52.4 cd/m^2); the pattern was updated to a totally new pattern on each frame at 75 Hz. In the unadapted region, SRN, whose spatial parameters were identical to those of the DRN, was presented in order to equate the apparent contrast variance with the adapted region.[2] The background (27.7 deg × 20.8 deg) was a uniform gray field (23.5 cd/m^2). In the test period, a totally new pattern of SRN covered the two regions.

Three seconds prior to the adaptation period, the fixation point appeared with a beep sound. Then came the stimulus, to which the subject simply adapted while keeping fixation. After 30 s of adaptation the test stimulus appeared and stayed stationary for 20 s. The total duration of the perceived visual jitter during the test period was timed; the subject pressed a button on the computer mouse if jitter was perceived and released it if not, and did so as many times as necessary.[3] The inter-trial interval was at least 10 s, during which the subject was allowed free eye movements.

[2] The presence or absence of SRN in the unadapted region during adaptation does not influence the duration of jitter illusion (Murakami & Cavanagh, 1998, Fig. 2).

[3] Despite this instruction, the subject rarely pressed the button more than twice in each trial.

Because the duration of illusory jitter was a subjective judgment, it is not meaningful to compare absolute values of duration across subjects. The absolute duration could also be influenced by the stimulus configurations in each experiment. However, the subject was urged to maintain the same criterion within each experiment, in which the independent variable(s) was (were) randomly varied from trial to trial.

3. Results

3.1. Storage

The storage phenomenon has been well documented in several aftereffect phenomena including the motion aftereffect: even if an intervening period longer than the typical duration of aftereffect is inserted between adaptation and test, a weaker but significant aftereffect is still obtained in the test (Wohlgemuth, 1911; Spigel, 1960, 1962, 1964; Wiesenfelder & Blake, 1990, 1992; Verstraten, Fredericksen, Grüsser, & van de Grind, 1994; Verstraten, Fredericksen, van Wezel, Lankheet, & van de Grind, 1996). Some take storage as evidence against a model of mere fatigue and recovery of detectors and as evidence for active control mechanisms adapting to a changing environment (Wiesenfelder & Blake, 1992; Thompson & Wright, 1994). Whatever the functional significance of storage may be, it is interesting to see if this particular characteristic of the motion aftereffect also manifests itself in visual jitter.

The adapted and unadapted regions were a disk (6.7 deg in diameter) and a surrounding annulus (6.7 deg in inner diameter and 13.3 deg in outer diameter), respectively (Fig. 1). The stimulus configuration was identical to that of the previous study (Murakami & Cavanagh, 1998). Between adaptation and test, a blank period of variable length was inserted, during which the monitor was kept completely black except for the fixation point.

Fig. 2 shows the total duration of visual jitter as a function of the blank interval. First of all, the duration of jitter decreased as the blank interval lengthened, not surprisingly. More importantly, jitter survived even though the inserted blank period was longer than the typical duration of jitter. This indicates that the effect of adaptation is somewhat stored during the blank period, after which it is finally discharged by the presence of a static test stimulus. Were there no storage, jitter should decrease solely as a function of time elapsed since the end of adaptation, no matter whether there was a blank period or not. In this case, the sum of the duration of jitter perceived following the blank interval and the duration of the blank interval should be constant. Such constraint lines are superimposed upon each profile. The data do not obey these lines. Instead, an exponential decay function well approxi-

mates the data. Thus, there is storage for visual jitter. In this respect, jitter is similar to motion aftereffect.

Where is the underlying mechanism of the storage of jitter located in the visual system? An anecdote in a subsidiary observation from a previous study on jitter (Murakami & Cavanagh, 1998) suggests a *monocular* storage site. When one eye was adapted and the other eye was tested, there was no interocular transfer. If the adapted eye was opened again at the end of such a trial, however, the observer often reported a bit of residual jitter that survived the test of the unadapted eye. This suggests that an effect of adaptation is stored monocularly and discharged only by the test stimulus presented in the adapted eye.

This observation differs in some aspects from the results seen for the motion aftereffect. In the study of Wiesenfelder and Blake (1992), between adaptation and test there was an intervening period, during which a stationary stimulus was presented in the adapted eye. With this, the motion aftereffect measured afterward was much weaker than without it, not surprisingly. However, when this intervening stimulus was made invisible by a binocularly rivalrous stimulus in the opposite eye, the aftereffect was stored just as if the stationary stimulus had been absent during the intervening period. On the one hand, this indicates that the underlying mechanism of the storage is affected by binocular interaction, thus located at a binocular stage (Spigel, 1964). On the other hand, this result does not rule out the existence of other, earlier sites of adaptation/storage. Thus, it is probable that there are multiple, monocular and binocular, adaptation sites for motion aftereffect, only the earlier of which is shared with visual jitter. That there is partial interocular transfer of motion aftereffect whereas there is none in the case of jitter (Barlow & Brindley, 1963; Murakami, 1995; Murakami & Cavanagh, 1998), also suggests that the shared site is monocular.

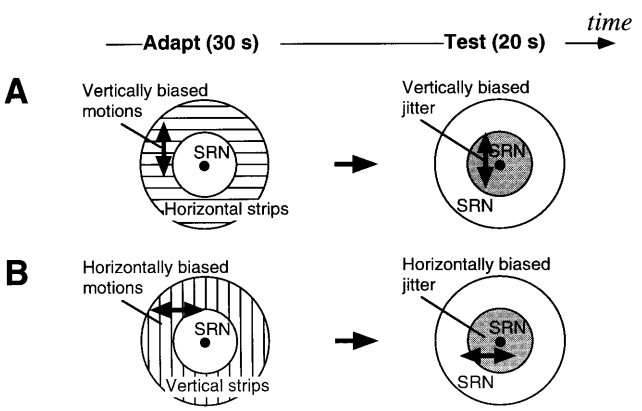

Fig. 3. Schematics of the stimulus configuration and typical percept in the demonstration of directional selectivity. In the adaptation period, static random noise (SRN) was presented within the center disk, whereas there was dynamic random noise (DRN) in the surrounding annulus. (A) The horizontal-strip version. The dynamic noise consisted of horizontal strips, each of which was assigned black or white randomly at each frame. This pattern contains motion energy biased toward vertical, and actually yields vivid impressions of randomly oscillating vertical motions. (B) The vertical-strip version.

3.2. Directional selectivity

The previous finding, together with the lack of interocular transfer of visual jitter (Murakami & Cavanagh, 1998), suggests the existence of a monocular adaptable neural site with storage capacity. Anatomically, the possible candidates for such monocular stages along the thalamic pathway of the primate would include the retina, lateral geniculate nucleus (LGN), and monocularly driven neurons in early cortical areas such as primary visual cortex (V1). Of these, directional selectivity of single cells first emerges in V1 (Hubel & Wiesel, 1968). This physiological landmark raises an interesting question: is visual jitter directionally selective? If it is, directionally selective mechanisms must be involved in neural adaptation, which implies the involvement of the cortex. The next demonstration shows that this is indeed the case.

SRN was presented within a disk-shaped unadapted region (6.7 deg in diameter) while an adapting stimulus was presented in the surrounding annulus (6.7 deg in inner diameter and 13.3 deg in outer diameter). The spatial relationship between the adapted and unadapted regions was now opposite to that of the previous experiment; this particular stimulus configuration, for which jitter was also vividly seen (Murakami & Cavanagh, 1998, Fig. 1), was chosen because the direction of jitter was easiest to discern in the central portion of the visual field. Were the adapting stimulus DRN, an isotropic visual jitter aftereffect would be seen, i.e. illusory motion could be in any direction reflecting the random nature of small eye movements. However, the adapting stimulus used in this experiment was one-dimensional DRN that effectively introduced a directional bias (Fig. 3). That is, the dots along the same horizontal (or vertical) level had the same luminance value, such that the pattern consisted of horizontal (or vertical) strips, each of which was assigned black or white in random fashion at each frame. Such a stimulus contains no motion energy along the horizontal (or vertical) axis, therefore biasing the directions of adaptation toward vertical (or horizontal). The test stimulus was static two-dimensional random noise as used in the previous experiment. The subject was asked to report which direction was more predominant in perceived jitter, i.e. horizontal or vertical.

More than five subjects observed the horizontal-strips version and the vertical-strips version at least twice each. They always reported that after adaptation

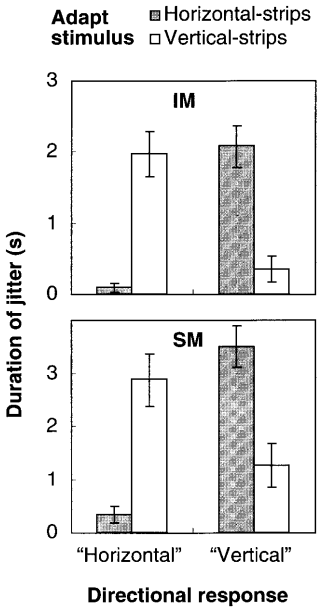

Fig. 4. The directional selectivity of visual jitter. The total duration of horizontally-biased jitter and vertically-biased jitter (mean ± 1 S.E. of 16 repeats) is plotted in the left-hand and right-hand columns, respectively. Within each column, duration is plotted separately according to the version of stimulus provided to the tested eye during adaptation. The data of the first author and a naive subject are shown in separate panels.

to the horizontal-strips version (which produces vertical motions), vertical jitter was predominant, and vice versa for the vertical-strips version (Fig. 3). Also, watching a screen demonstration of this, more than 100 observers in the audience of a conference presentation confirmed this perceptual bias, with only a couple of nays (Murakami & Cavanagh, 1999).

The adapting stimulus contains a clearly visible orientation cue that could potentially work as a cognitive bias, especially if a clever subject has learned the association between the adapting stimulus and subsequent percept. To overcome this problem, we dichoptically presented two different adapting stimuli via a mirror haploscope: one eye received the horizontal-strips version and the other eye received the vertical-strips version. Perceptually, binocular rivalry occurred where the orthogonally oriented gratings were superimposed. The subject reported that the two rivalrous images appeared in alternation at equal probabilities. After adaptation, the test stimulus was provided to only one eye. The trick is that the subject did not know which version of adapting stimulus this eye had received beforehand. While jitter was perceived, the subject was asked to press one of the two, 'horizontal' and 'vertical', arrow keys of the computer (and to switch back and forth if necessary), depending on which direction was more predominant. The total duration of jitter was separately calculated for the two directional responses.

Fig. 4 shows the 'horizontal' duration and 'vertical' duration plotted separately according to which version of adapting stimulus had been presented to the tested eye. Clearly, the horizontal-strips version resulted in much more 'vertical' than 'horizontal' responses, and vice versa. The overall duration was shorter than usual, but it was inevitably so because binocular rivalry ought to halve the effective duration of adaptation and because switching between the two keys in the subject's motor behavior introduces considerable loss in time (i.e. while neither key was pressed at each switching, the subject could have been observing clear jitter, to which the subject would have kept pressing the button in a usual duration measurement).

This result confirms the informal observations described above. Furthermore, the present data offer additional evidence for the monocular nature of adaptation. Binocular stages always received the mixture (or rivalry) of both versions during adaptation, no matter which eye was tested subsequently. Therefore, binocular stages are ruled out as the basis of these eye-specific differential responses.

In short, visual jitter tends to occur along the directional axis that is most adapted. As such, jitter exhibits directional selectivity. Adaptation in the retina or LGN cannot explain this, because, in primates, neurons in these sites only have isotropic receptive fields (RFs) without sensitivity for orientation or direction. Thus, some cortical adaptation must be postulated in order to explain the direction-specific effect of visual jitter. But why vertically biased jitter after vertically biased adaptation? After adaptation, directionally selective mechanisms tuned to vertical have been more adapted than others. As a result, vertical retinal slip is more severely underestimated, whereas horizontal slip is more properly processed by unattenuated mechanisms. Thus, vertical slip results in more vigorous jitter than horizontal.

As oriented stimuli were used, one might argue that the present result only indicates selectivity for orientation, instead of direction. In either case, however, the main conclusion is the same, because both orientation selectivity and directional selectivity first emerge at the level of V1. If jitter exhibits selective adaptation for orientation, or for direction, or for their interaction, all suggest the involvement of the cortex.

That V1 should be involved in adaptation, however, does not preclude the involvement of adaptation prior to the cortex. Indeed, DRN contains spatiotemporal frequencies suitable for driving cells in the retina and LGN, the magnocellular subsystem in particular (Livingstone & Hubel, 1987). Thus, the retinal ganglion cells, LGN cells, and V1 cells are probably all adapted to a certain extent, but among V1 cells directionally biased stimuli induce some inhomogeneity in adaptation, which results in directionally biased jitter.

3.3. Spatial frequency selectivity

Next, we examined if there is any effect of spatial frequency like that exhibited by the motion aftereffect:

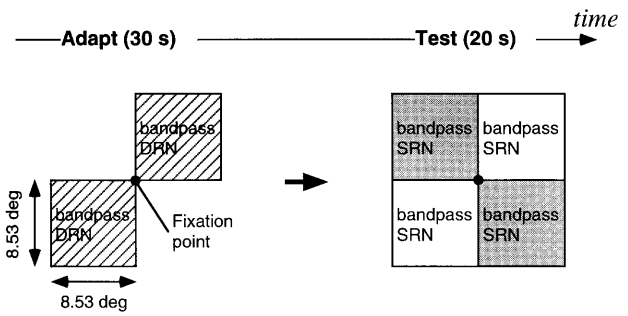

Fig. 5. A schematic of the experiment that assessed spatial frequency selectivity. During adaptation, two bandpass filtered images were presented in diagonal fashion. Independent patterns were presented successively from frame to frame. The unadapted regions were left unstimulated. During test, four bandpass filtered images were presented statically in the adapted and unadapted regions. The passbands of adapting and test stimuli were chosen randomly among the five possible values.

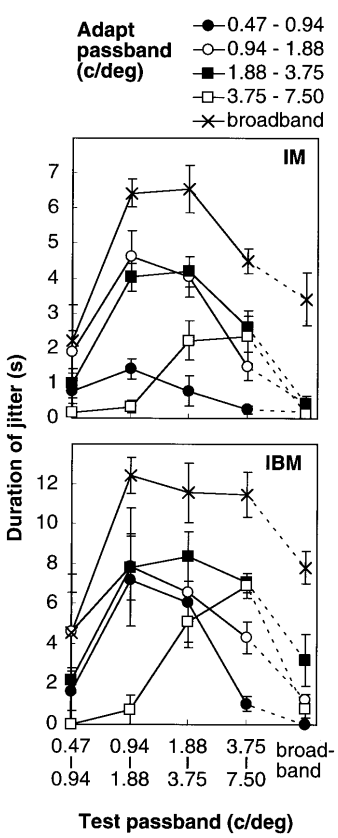

Fig. 6. The spatial frequency selectivity of visual jitter. The total duration of visual jitter (mean ± 1 S.E. of four repeats) is plotted against the passband of the test stimulus, with the passband of the adapting stimulus as a parameter. The data of the first author and a naive subject are plotted in separate panels. Indicated as 0.47–0.94, for instance, are the low and high cutoff frequencies. 'Broadband' indicates unfiltered random noise as used in other experiments.

the more similar the spatial frequency components between the adapting and test stimuli, the stronger the aftereffect (Over, Broerse, Crassini, & Lovegrove, 1973; Cameron, Baker, & Boulton, 1992; Ashida & Osaka, 1994; Bex, Verstraten, & Mareschal, 1996; Mareschal, Ashida, Bex, Nishida, & Verstraten, 1997). It was demonstrated that this is also the case in visual jitter, using bandpass filtered random noise patterns.

We made use of a standard bandpass filtering protocol (e.g. Nishida & Sato, 1992). A square (256 pixels × 256 pixels) of black and white random noise pattern was generated (1 dot = 1 pixel), Fourier-transformed into the frequency domain, filtered, and finally inverse-Fourier-transformed into the spatial domain. An annular filter centered in the frequency domain removed all frequency components outside it, preserving all components inside. Each filter had a 1-octave bandpass window. Four different spatial frequency passbands were used (see Fig. 6). The unfiltered random dot pattern as used in the previous experiments (1 dot = 4 × 4 pixels) was also used. Hence, there were five varieties of stimuli in total. The adapted and unadapted regions were arranged as shown in Fig. 5. In the adapted regions, bandpass filtered random noise patterns were displayed dynamically.[4] The unadapted regions were left blank in order to keep these regions neutral with respect to spatial frequency during adaptation. The fixation point was provided at the center. The subject adapted to this display for 30 s, after which the test stimuli, bandpass filtered images, were presented statically at all of these four regions. The passbands of the adapting stimulus and the test stimulus were chosen in random order from the 5 × 5 factorial design.

Fig. 6 shows the total duration of visual jitter plotted against the test passband, with the adaptation passband as a parameter. 'Broadband' indicates the unfiltered random noise. First of all, visual jitter occurred even after adaptation to spatially filtered DRN. The illusion was considerably weaker, however, compared with the adaptation to unfiltered noise. Second, after adaptation to broadband noise, bandpass filtered test stimuli were more apt to jitter than the broadband test. For this particular stimulus configuration, the jitter in broadband-adapt, broadband-test condition was somewhat weaker than in other experiments. However, making the test stimulus bandpass strongly enhanced the illusion (except for the lowest passband). Taken together, filtered noise is less effective if used as the adapting stimulus, and more easily jitters if used as the test stimulus.

[4] One hundred and fifty independent images were prepared at each passband and presented sequentially. Thus, although the adapting stimulus was spatial frequency bandpass, its temporal-frequency power was still flat.

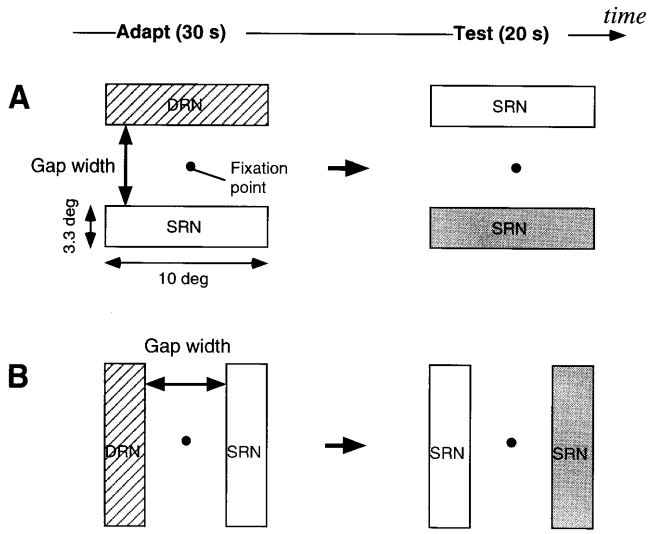

Fig. 7. A schematic of the experiment that assessed inter-hemifield transfer. During adaptation, dynamic random noise (DRN) was presented on one side, whereas static random noise (SRN) was presented on the other side. Both regions were static during test. The distance between the two regions was variable. (A) Within-hemifield condition, in which both adapted and unadapted regions were in the same lateral hemifield. (B) Inter-hemifield condition, in which the adapted region was in the left (or right) hemifield and the unadapted region was in the right (or left) hemifield.

The third point, which we think is most important, is that visual jitter was greatest when the passbands of the adapting and test stimuli matched. Such spatial frequency selectivity is readily observed at all spatial frequency passbands, except for the lowest one (filled circles), at which the greatest jitter was obtained at the next lowest range. Overall, again, visual jitter shows remarkable similarity to motion aftereffect (Over et al., 1973; Cameron et al., 1992; Ashida & Osaka, 1994; Bex et al., 1996; Mareschal et al., 1997). The shift of optimal spatial frequency at the lowest passband also looks similar to what Cameron et al. observed in their motion aftereffect study: adaptation to a 0.25 c/deg sinusoidal grating yielded the greatest motion aftereffect at the 0.5 c/deg test grating, not 0.25 c/deg. The authors attributed this peak shift to the tuning of the lowest spatial frequency channel at the tested retinal eccentricity (4 deg) — this account is not only found plausible but also applicable to the current results.[5] These similarities between motion aftereffect and visual jitter in terms of spatial frequency selectivity suggest that the two illusions share common mechanisms at early stages of motion processing.

3.4. Inter-hemifield transfer

It has been shown that the effect of adaptation is monocular (Murakami & Cavanagh, 1998), stored, directionally selective to some extent, and spatial frequency selective. These characteristics suggest that the adaptable site is located at fairly early stages such as monocularly driven directionally selective cells in V1. The next two experiments address the other main question: where is the compensation stage (see Section 1) located in the brain? Knowledge about cortical architecture may help. At the level of V1 and earlier, the left hemifield is represented almost exclusively in the right hemisphere and vice versa, with minimal interaction between the hemispheres (Kennedy & Dehay, 1988). Also, the RF diameters of single neurons are in the order of minutes of arc. In contrast, more specialized motion areas (MT, MST, and higher) have richer transcallosal connections (Van Essen, Newsome, & Bixby, 1982). Also, individual cells in these areas generally have larger RFs that often invade the ipsilateral visual field (e.g. for MT, Gattass & Gross, 1981; Raiguel, Van Hulle, Xiao, Marcar, & Orban, 1995; Raiguel, Van Hulle, Xiao, Marcar, Lagae, & Orban, 1997). Fairly large ipsilateral representation in human MT + has also been reported (Tootell, Reppas, Kwong, Malach, Born, Brady, Rosen, & Belliveau, 1995). Therefore, an interesting question is whether visual jitter transfers between hemifields.

For the *within*-hemifield transfer test, the adapted and unadapted regions were horizontally oriented rectangles (10 deg × 3.3 deg), vertically apart (Fig. 7A). For the *inter*-hemifield transfer test, they were vertically oriented rectangles, horizontally apart (Fig. 7B). In both conditions, the fixation point was provided at the midpoint between the two regions. The background was black, and spatial cues from environment was eliminated by using a cardboard-made 'tunnel' between the monitor and the observer, in order to ensure that the adapted and unadapted regions should be the nearest visible objects to each other.

Fig. 8 shows the total duration of visual jitter as a function of the distance between the adapted and unadapted regions (designated 'gap width'). For *within*-hemifield condition, visual jitter decreased with increasing the distance, as expected. However, the effect of adaptation still persisted even when the adapted and unadapted regions were separated by up to 6, 7, and 5 deg for subjects IM, YS, and DW respectively.[6] Evidently, purely local accounts, such as processing within the classical RFs of single cells in V1, fail to explain the results, because the V1 RF (2 deg wide at best) cannot

[5] Parts of the stimuli were more foveal than 4 deg, which presumably produced the peak shift at a higher spatial frequency portion than Cameron et al.'s results.

[6] Beyond these points, *t*-tests did not reveal a significant difference from the duration of 1 s, which we take as a conservative criterion of the presence of jitter.

bridge across the two regions apart this far (Gattass & Gross, 1981).

Cooperativity within V1 might propagate motion signals across such a long distance despite small RFs of individual cells. For example, long range horizontal connections of axon collateral observed in V1 might do this job (Ts'o, Gilbert & Wiesel, 1986). However, the results of the *inter*-hemifield condition make it unlikely. They appear almost indistinguishable from the data of the within-hemifield condition, although the overall level of duration is a little bit shorter. The adapted and unadapted regions could be separated as far as 5, 6, and 2 deg for IM, YS, and DW, respectively, to elicit jitter. For jitter to transfer across these lengths, intimate conversation between the two hemispheres is necessary — V1 does not seem the most likely place to find these connections. The surprisingly great extent of inter-hemifield transfer of visual jitter, therefore, favors the idea of extrastriate contribution to retinal-slip compensation.

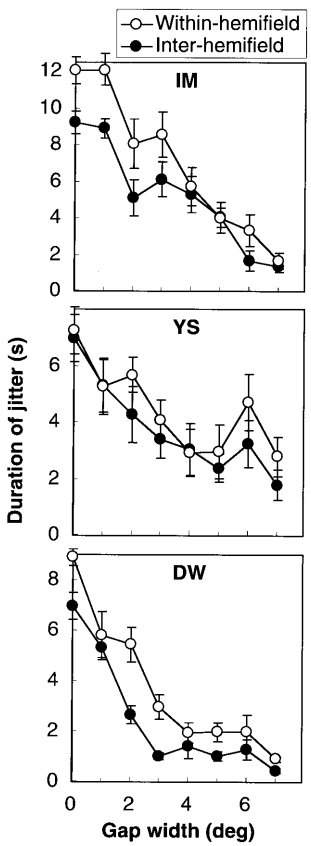

Fig. 8. The inter-hemifield transfer of visual jitter. The total duration of visual jitter (mean ± 1 S.E. of 6–10 repeats) is plotted against gap width, i.e. the distance between the adapted and unadapted regions. Each panel corresponds to each subject (the first author and two naive subjects participated; all had corrected-to-normal vision). The data in the within-hemifield condition are plotted as ○, whereas the data in the inter-hemifield condition are plotted as ●.

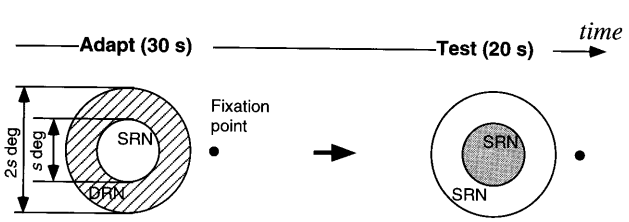

Fig. 9. A schematic of the experiment that assessed stimulus size specificity. The sizes of dynamic random noise (DRN) and static random noise (SRN) were manipulated by variable *s*.

3.5. Stimulus size specificity

The extent of the inter-hemifield transfer implicates extratriate areas but it does not resolve which of these areas might be responsible. Estimating the optimal stimulus size for visual jitter is of great interest in this context because RF sizes of neurons along motion processing pathway vary from area to area. In electrophysiological literature, the RF size is generally described as a function of eccentricity. Therefore, both the stimulus size and eccentricity were varied in this experiment in order to evaluate this potential signature of the area mediating compensation.

The experiment was done in a dark room with only negligible ambient light. The unadapted and adapted regions were a disk (*s* deg in diameter, where *s* is a variable size parameter, see Fig. 10) and a surrounding annulus (*s* deg in inner diameter and 2*s* deg in outer diameter), respectively (Fig. 9). For this stimulus configuration, it was possible to measure the duration over the greatest range with least error. The observation was made at several eccentricities by placing the horizontal location of the fixation point at different distances to the right of the stimulus. The parameter *s* was varied by redrawing the stimulus at the desired size in each trial. The eccentricity and stimulus size were chosen in random order within each session.

In Figs. 10 and 11, the total duration of visual jitter is plotted against center diameter *s* indicated along the upper abscissa of each panel. Each panel shows the results for one eccentricity. At 1 deg eccentricity, the duration was roughly flat irrespective of stimulus size (filled circles). In contrast, the data at 9-deg eccentricity showed an increasing function of stimulus size (filled inverted triangles). Both aspects were observed in the data at 3-deg eccentricity and others. This suggests that a rising then saturating function is a generic form of stimulus size dependence of visual jitter. The different profiles at each eccentricity can be superimposed by horizontally shifting versions of this generic form.

In each panel, the data was first plotted at the midpoint eccentricity, namely 4.5 deg, with open circles. The lower abscissa indicates the center diameter *s* at this eccentricity. Next, the data was superimposed at the eccentricity of interest, for example 1 deg, onto the 4.5-deg data, with filled symbols. The second set of data

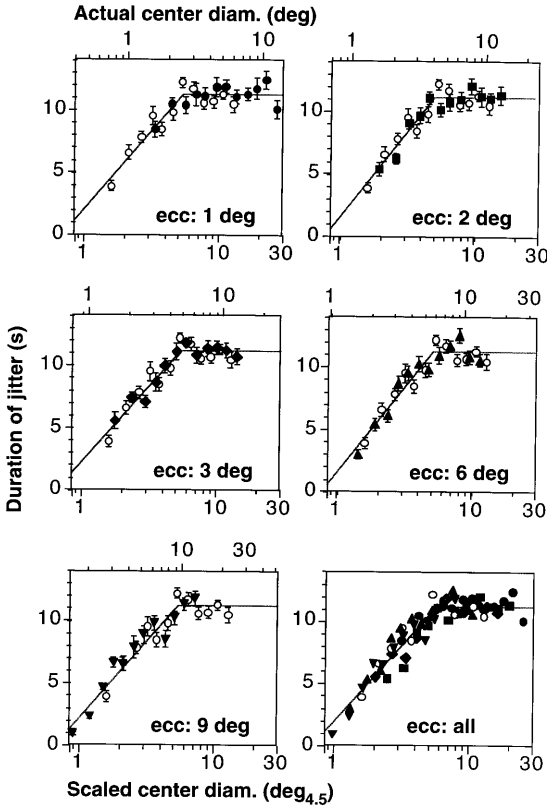

Fig. 10. The stimulus size specificity of visual jitter, the first author IM's data. The total duration of visual jitter (mean ± 1 S.E. of 16 repeats) is plotted against stimulus size. The upper abscissa of each panel indicates actual center diameter, s, in deg. The data at each eccentricity are plotted with filled symbols. Superimposed upon them are the data at 4.5 deg eccentricity, with ○, which are plotted against the lower abscissa that indicates the center diameter at this eccentricity (designated $\deg_{4.5}$, meaning stimulus size in deg at 4.5 deg eccentricity). The data for a given eccentricity are shifted horizontally so that they appear to align with the 4.5 deg data. The lower right panel shows the plot of all the data scaled according to the estimated factor.

was then translated horizontally along the logarithmic axis so that the two profiles appear to collapse into a single function.[7]. In Fig. 10, the data at 1 deg eccentricity, for example, had to be shifted rightward by 0.32 log unit (see the discrepancy between the lower and upper abscissae); the data at 9 deg eccentricity had to be shifted leftward by 0.25 log unit. Overall, the estimated amount of shift changed systematically as a function of eccentricity. The amount of rightward shift expressed as $\log(1/f)$, f was fit to a linear increasing function of eccentricity, $f = 1 + 0.141\ (E - 4.5)$ for subject IM and $f = 1 + 0.132\ (E - 4.5)$ for SM, where E denotes eccentricity. This equation was used to plot all the data on the lower right panel. The data appear to be well described by a single function. Thus, the strength of visual jitter can be expressed as a function of scaled size irrespective of eccentricity. Furthermore, from this summarized diagram one can estimate the critical center diameter, at which an increasing slope just reaches an asymptote: $2.08\ (1 + 0.386E)$ deg for IM and $2.10\ (1 + 0.325E)$ deg for SM. This function will be used to select a candidate area that mediates the compensation of small retinal motion during fixation.

[7] The least-square method was used to estimate a set of parameters that minimize the residuals of fit to a linear function with saturation, $y = \min(ax + b,\ c)$; a, b, c, and the amount of horizontal shift were variable parameters. However, the choice of the form of the function did not significantly alter the estimation of scaling factors.

4. Discussion

4.1. Two distinct stages involved in visual jitter

The present study has revealed two distinct stages underlying the visual jitter aftereffect: adaptation and compensation. The effect of adaptation shows storage, directional selectivity, and spatial frequency selectivity. These characteristics resemble the characteristics of motion aftereffect, thus suggesting some overlap in the adaptation mechanisms for the two effects. Taken together with the previous result that there is no interocular transfer (Murakami & Cavanagh, 1998), which indicates that adaptation is primarily monocular, it is

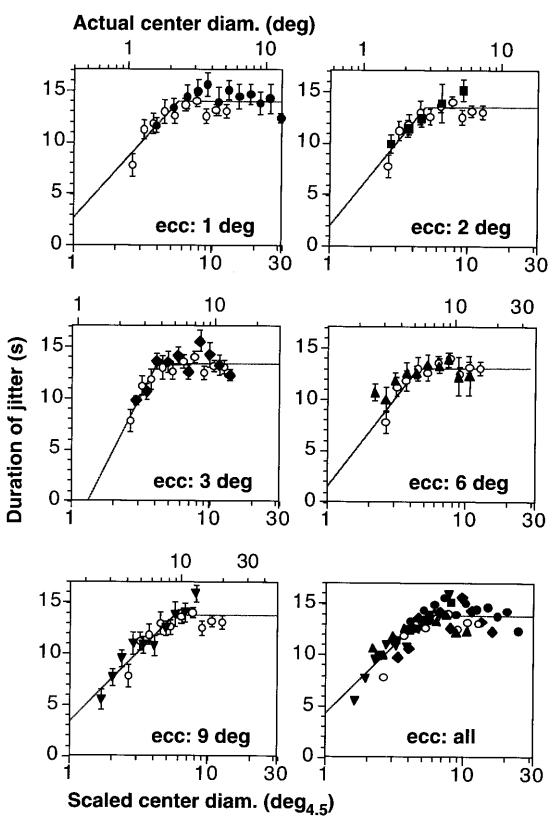

Fig. 11. The stimulus size specificity of visual jitter, naive subject SM's data. The total duration of visual jitter (mean ± 1 S.E. of 6–10 repeats) is plotted against stimulus size.

likely that the first stage of visual jitter is located at an early stage of motion processing, where direction- and spatial frequency- selective monocular units are located. One of the best candidates for such a stage in the primate visual cortex is V1 layer 4B, although the directionally selective bias per se does not necessarily preclude the involvement of prior stages such as magnocellular LGN.

In contrast, the data suggest that the second stage is located considerably later, where information can be compared across the left and right hemispheres. The scarce transcallosal connections in V1 do not seem a likely source for the inter-hemifield transfer that was observed — richer connectivity in higher extrastriate areas would be required (Van Essen et al., 1982; Kennedy & Dehay, 1988). Further, the minimum stimulus size required to give rise to the maximum visual jitter was found to scale as a linear function of eccentricity just like the RF size of cortical neurons does. Quantitatively, this critical stimulus size mimics the RF size of MT neurons (as discussed later). It seems that these results can be viewed as converging evidence for a higher site for the compensation process.

4.2. Related psychophysical work

Retinal slip due to eye movements is normally kept unseen. It is perceived only when the compensation mechanism is perturbed, in this case by adaptation to DRN. There are two other interesting cases, both involving stabilized images, wherein retinal slip is made visible.

An afterimage, if small enough, normally appears to move with the eye. However, when a large object is briefly flashed in complete darkness, its afterimage can look very stable (Power, 1983; Pelz & Hayhoe, 1995). In this case, an LED that is stationary in the outer world — therefore moving on the retina with eye movements — appears to move. Clearly, attribution of 'frame of reference' to larger objects determines which pattern (afterimage or LED) should appear to move. In terms of our theory, the minimum motion will be that of the elements of the afterimage so the LED's motion should not only show large shifts with gross drifts in gaze but should also appear to jitter as a result of small, rapid eye movements. This prediction is currently being examined.

Motion of a small target is detected more easily on a textured background than when the target is presented alone. However, image stabilization of the textured background elevates the motion detection threshold of the central target, presumably because the retinal slip added to the target motion can no longer be subtracted by the compensation mechanism. Retinal slip is now added in as noise jittering in random directions, relative to completely stable background (Tulunay-Keesey & VerHoeve, 1987). This is essentially similar to the aforementioned case of a small LED surrounded by a large afterimage. These observations are incompatible with extraretinal theories but favor the visual-motion-based model.

4.3. Biological implementation of retinal-slip compensation

In order to reduce the metabolic cost of incessant responses to retinal slip, one would imagine that the effects of eye movements would be corrected as soon as possible. However, neurons in early cortical areas such as V1 respond to retinal slip as readily as to object motion (Galletti et al., 1984; Gur & Snodderly, 1987, 1997; Ilg & Thier, 1996; Gur et al., 1997; Leopold & Logothetis, 1998; Gur, Beylin, & Snodderly, 1998; Martinez-Conde, Macknik & Hubel, 2000). Thus, V1 responses seem a simple copy of what is happening on the retina. A similar tendency may hold for various areas along the parietal pathway before MST (Erickson & Thier, 1991; Gur & Snodderly, 1997; Ilg, 1997; Bair & O'Keefe, 1998; Shenoy, Bradley, & Andersen, 1999), though some have claimed that a fraction of cells in earlier areas are already clever enough to fire only at 'real motion' (Galletti et al., 1984; Galletti, Battaglini, & Aicardi, 1988; Galletti, Battaglini, & Fattori, 1990).

In Section 1, it was argued that these spurious motion responses elicited by eye movements can be canceled by vector subtraction using the minimum vector as a baseline. Mathematically equivalent, but biologically more efficient solutions can be considered. For example, neural units only responsive to purely relative motion might do a good job, as they would keep silent upon common image motion due to eye movements. However, the outputs of such hypothetical units could not tell which region, the adapted one or the unadapted one, ought to move in visual jitter (Murakami & Cavanagh, 1998). The observation is that the adapted region, where motion sensitivity is reduced, invariably appears stationary, whereas the unadapted region is seen to move together with one's eye movements.

We would argue that this reflects the characteristics of silent surround suppression as seen in several areas, MT in particular (Allman, Miezin, & McGuinness, 1985a; Allman, Miezin & McGuinness, 1985b, 1990; Tanaka, Hikosaka, Saito, Yukie, Fukada, & Iwai, 1986; Lagae, Gulyás, Raiguel, & Orban, 1989; Born & Tootell, 1992; Xiao, Raiguel, Marcar, Koenderink, & Orban, 1995; Hupé, James, Payne, Lomber, Girard, & Bullier, 1998). They behave like relative motion cells, in that common image motion is not a good stimulus for them. Instead, they fire when motion in the preferred direction covers the RF center and a static pattern covers the suppressive surround. However, they do not respond to an equivalent relative motion when the

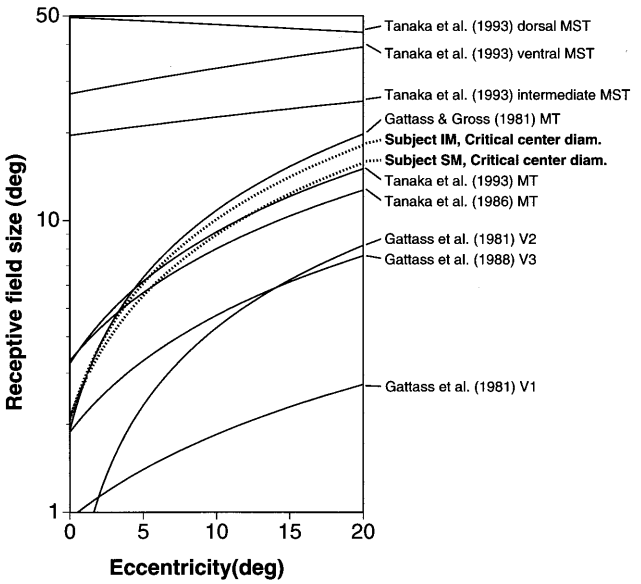

Fig. 12. The relationship among the critical center diameter of the present study and RF sizes (square root of RF area) of several cortical areas of the macaque.

center receives a stationary pattern and the surround receives motion in the antipreferred direction. Thus, these units are not 'purely relative motion' cells. Such asymmetry in the response property may qualitatively help assign motion and stationarity to appropriate regions of the visual field. Finally, more global process computing perceptual stability may be at work in addition to such local interactions: the factors of 'enclosure' and 'frame of reference' may be sometimes crucial for unconsciously inferring what should be moving with respect to what (Power, 1983; Pelz & Hayhoe, 1995).

4.4. The implication of the critical stimulus size

If the compensation in the model is in fact implemented in the form of RFs with suppressive surrounds, the optimal stimulus size for eliciting visual jitter might then be such that the stimulus center falls onto the classical RF while the stimulus surround does not invade it. Too small a stimulus would make the motion difference between stimulus center and surround below the resolution limit. Larger than optimal stimuli would become less effective for a single cell, but at the same time they would recruit more cells with various size tunings and RF locations, making the eccentricity control less precise. These respective situations might correspond to the ascent and saturation of the Figs. 10 and 11.

Thus, it is interesting to compare the optimal stimulus size for visual jitter with RF sizes of several cortical areas. In Fig. 12, the critical center diameter estimated from the data is plotted against eccentricity. Superimposed are regressions of classical RF sizes of neurons in the macaque V1, V2, V3, MT, and MST (Gattass & Gross, 1981; Gattass, Gross, & Sandell, 1981; Gattass, Sousa, & Gross, 1988; Tanaka et al., 1986; Tanaka, Sugita, Moriya, & Saito, 1993). Clearly, the critical center diameter resembles the typical RF size of macaque MT neurons with a surprising order of similarity, especially within the tested eccentricity range (1–9 deg). That of V1 neurons is much smaller by one log unit, whereas that of MST neurons is much larger by one log unit.[8]

There are a few additional electrophysiological reports that suggest the contribution of other areas. Many neurons in the ventral part of MST, which is one of the recipients of MT outputs, exhibit some form of center-surround antagonism and have RFs that could be as small as those of typical MT neurons (Komatsu & Wurtz, 1988; Tanaka, Sugita, Moriya, & Saito, 1993; Eifuku & Wurtz, 1998). Also, the superficial layers of superior colliculus have been reported to contain many cells that are suppressed when there is no relative motion between the inside and outside of the RF (whose size is only 1/3 of those of typical MT cells), irrespective of absolute direction or speed (Bender & Davidson, 1986; Davidson & Bender, 1991). Thus, it is possible that these loci are playing some important role in the compensation process of the model. Interestingly, inactivating MT abolishes the motion opponency of superior colliculus neurons (Davidson, Joly & Bender, 1992; Joly & Bender, 1997) and, to a lesser extent, V1, V2, and V3 neurons too (Hupé et al., 1998). These results suggest that MT generates and outputs multipurpose motion opponent signals, some of which are used for eye-movement compensation in MT itself as well as elsewhere.

Does the compensation process for visual jitter share a common underlying mechanism with other psychophysical motion tasks related to relative motion processing? Previous studies have shown that such visual tasks exhibit smaller critical stimulus sizes, which increase more steeply with increasing eccentricity (Levi,

[8] This argument relies upon the assumption of the macaque monkey as an ideal animal model of humans, whose RF data are inaccessible by current physiological technique. In fact, accumulating lines of evidence indicate interspecies similarities in several respects. First, animal psychophysics has demonstrated that monkeys and humans have the same motion detection performance (Golomb, Andersen, Nakayama, MacLeod, & Wong, 1985; Newsome, Britten, & Movshon, 1989). Second, functional magnetic resonance imaging has revealed human cortical hierarchy homologous to the above-mentioned monkey visual areas (Sereno, Dale, Reppas, Kwong, Belliveau, Brady, Rosen, & Tootell, 1995). Third, psychophysical approaches to estimating the RF of human motion detectors argue for similarities in RF sizes between the two species (Johnston & Wright, 1986; Anderson & Burr, 1987; Burr, Morrone, & Vaina, 1998). Nevertheless, we would also like to note that none of the above arguments rejects a hypothesis that all the apparent similarity between the data and the MT's RF data is coincidental.

Klein & Aitsebaomo, 1984; McKee & Nakayama, 1984; Murakami & Shimojo, 1995, 1996). This suggests that the *perception* of relative motion requires some other machinery than that used in the compensation of retinal slip. This apparent dissociation is currently under study.

Acknowledgements

Pilot experiments of this research were presented elsewhere (Murakami & Cavanagh, 1999, 2000). Part of this research was conducted while the first author was a post-doctoral fellow at Department of Psychology, Harvard University. Preparation of this article was supported by NIH grants EY09258 (to PC). We would like to thank Yoh'ichi Tohkura, Kenichirou Ishii, Seiichiro Naito, Norihiro Hagita, and Tatsuya Hirahara of NTT Communication Science Laboratories for their support.

References

Allman, J., Miezin, F., & McGuinness, E. (1985a). Direction- and velocity-specific responses from beyond the classical receptive field in the middle temporal visual area (MT). *Perception*, *14*, 105–126.

Allman, J., Miezin, F., & McGuinness, E. (1985b). Stimulus specific responses from beyond the classical receptive field: neurophysiological mechanisms for local-global comparisons in visual neurons. *Annual Review of Neuroscience*, *8*, 407–430.

Allman, J., Miezin, F., & McGuinness, E. (1990). Effects of background motion on the responses of neurons in the first and second cortical visual areas. In G. M. Edelman, W. E. Gall, & W. M. Cowan, *Signal and Sense: Local and Global Order in Perceptual Maps* (pp. 131–141). New York: Wiley.

Anderson, S. J., & Burr, D. C. (1987). Receptive field size of human motion detection units. *Vision Research*, *27*, 621–635.

Ashida, H., & Osaka, N. (1994). Difference of spatial frequency selectivity between static and flicker motion aftereffects. *Perception*, *23*, 1313–1320.

Bair, W., & O'Keefe, L. P. (1998). The influence of fixational eye movements on the response of neurons in area MT of the macaque. *Visual Neuroscience*, *15*, 779–786.

Barlow, H. B., & Brindley, G. S. (1963). Inter-ocular transfer of movement aftereffects during pressure blinding of the stimulated eye. *Nature*, *200*, 1347–1347.

Bender, D. B., & Davidson, R. M. (1986). Global visual processing in the monkey superior colliculus. *Brain Research*, *381*, 372–375.

Bex, P. J., Verstraten, F. A. J., & Mareschal, I. (1996). Temporal and spatial frequency tuning of the flicker motion aftereffect. *Vision Research*, *36*, 2721–2727.

Born, R. T., & Tootell, R. B. H. (1992). Segregation of global and local motion processing in primate middle temporal visual area. *Nature*, *357*, 497–499.

Burr, D. C., Morrone, M. C., & Vaina, L. M. (1998). Large receptive fields for optic flow detection in humans. *Vision Research*, *38*, 1731–1743.

Cameron, E. L., Baker, C. L., Jr, & Boulton, J. C. (1992). Spatial frequency selective mechanisms underlying the motion aftereffect. *Vision Research*, *32*, 561–568.

Davidson, R. M., & Bender, D. B. (1991). Selectivity for relative motion in the monkey superior colliculus. *Journal of Neurophysiology*, *65*, 1115–1133.

Davidson, R. M., Joly, T. J., & Bender, D. B. (1992). Effect of corticotectal tract lesions on relative motion selectivity in the monkey superior colliculus. *Experimental Brain Research*, *92*, 246–258.

Ditchburn, R. W., & Foley-Fisher, J. A. (1967). Assembled data in eye movements. *Optica Acta*, *14*, 113–118.

Eifuku, S., & Wurtz, R. H. (1998). Response to motion in extrastriate area MSTl: center-surround interactions. *Journal of Neurophysiology*, *80*, 282–296.

Erickson, R. G., & Thier, P. (1991). A neuronal correlate of spatial stability during periods of self-induced visual motion. *Experimental Brain Research*, *86*, 608–616.

Freeman, T. C. A. (1999). Path perception and Filehne illusion compared: model and data. *Vision Research*, *39*, 2659–2667.

Freeman, T. C. A., & Banks, M. S. (1998). Perceived head-centric speed is affected by both extra-retinal and retinal errors. *Vision Research*, *38*, 941–945.

Galletti, C., Battaglini, P. P., & Aicardi, G. (1988). 'Real-motion' cells in visual area V2 of bahaving macaque monkeys. *Experimental Brain Research*, *69*, 279–288.

Galletti, C., Battaglini, P. P., & Fattori, P. (1990). 'Real-motion' cells in area V3A of macaque visual cortex. *Experimental Brain Research*, *82*, 67–76.

Galletti, C., Squatrito, S., Battaglini, P. P., & Maioli, M. G. (1984). 'Real-motion' cells in the primary visual cortex of macaque monkeys. *Brain Research*, *301*, 95–110.

Gattass, R., & Gross, C. G. (1981). Visual topography of striate projection zone (MT) in posterior superior temporal sulcus of the macaque. *Journal of Neurophysiology*, *46*, 621–638.

Gattass, R., Gross, C. G., & Sandell, J. H. (1981). Visual topography of V2 in the macaque. *Journal of Comparative Neurology*, *201*, 519–539.

Gattass, R., Sousa, A. P. B., & Gross, C. G. (1988). Visuotopic organization and extent of V3 and V4 of the macaque. *Journal of Neuroscience*, *8*, 1831–1845.

Golomb, B., Andersen, R. A., Nakayama, K., MacLeod, D. I. A., & Wong, A. (1985). Visual thresholds for shearing motion in monkey and man. *Vision Research*, *25*, 813–820.

Grüsser, O.-J., Krizič, A., & Weiss, L.-R. (1987). Afterimage movement during saccades in the dark. *Vision Research*, *27*, 215–226.

Gur, M., Beylin, A., & Snodderly, D. M. (1997). Response variability of neurons in primary visual cortex (V1) of alert monkeys. *Journal of Neuroscience*, *17*, 2914–2920.

Gur, M., Beylin, A., & Snodderly, D. M. (1998). Effects of fixational eye movements on cells in V1 of alert monkeys. *Society for Neuroscience Abstracts*, *24*, 1981.

Gur, M., & Snodderly, D. M. (1987). Studying striate cortex neurons in behaving monkeys: benefits of image stabilization. *Vision Research*, *27*, 2081–2087.

Gur, M., & Snodderly, D. M. (1997). Visual receptive fields of neurons in primary visual cortex (V1) move in space with the eye movements of fixation. *Vision Research*, *37*, 257–265.

Helmholtz, H. V. (1866). *Handbuch der physiologischen Optik*. Leipzig: Voss.

Hubel, D. H., & Wiesel, T. N. (1968). Receptive fields and functional architecture of monkey striate cortex. *Journal of Physiology*, *195*, 215–243.

Hupé, J. M., James, A. C., Payne, B. R., Lomber, S. G., Girard, P., & Bullier, J. (1998). Cortical feedback improves discrimination between figure and background in V1, V2 and V3 neurons. *Nature*, *394*, 784–787.

Ilg, U. J. (1997). Responses of primate area MT during the execution of optokinetic nystagmus and afternystagmus. *Experimental Brain Research*, *113*, 361–364.

Ilg, U. J., & Thier, P. (1996). Inability of rhesus monkey area V1 to discriminate between self-induced and externally induced retinal image slip. *European Journal of Neuroscience*, *8*, 1156–1166.

Johnston, A., & Wright, M. J. (1986). Matching velocity in central and peripheral vision. *Vision Research*, *26*, 1099–1109.

Joly, T. J., & Bender, D. B. (1997). Loss of relative-motion sensitivity in the monkey superior colliculus after lesions of cortical area MT. *Experimental Brain Research*, *117*, 43–58.

Kennedy, H., & Dehay, C. (1988). Functional implications of the anatomical organization of the callosal projections of visual areas V1 and V2 in the macaque monkey. *Behavioural Brain Research*, *29*, 225–236.

Komatsu, H., & Wurtz, R. H. (1988). Relation of cortical areas MT and MST to pursuit eye movements. III. Interaction with full-field visual stimulation. *Journal of Neurophysiology*, *60*, 621–644.

Lagae, L., Gulyás, B., Raiguel, S., & Orban, G. A. (1989). Laminar analysis of motion information processing in macaque V5. *Brain Research*, *496*, 361–367.

Leopold, D. A., & Logothetis, N. K. (1998). Microsaccades differentially modulate neural activity in the striate and extrastriate visual cortex. *Experimental Brain Research*, *123*, 341–345.

Levi, D. M., Klein, S. A., & Aitsebaomo, P. (1984). Detection and discrimination of the direction of motion in central and peripheral vision of normal and amblyopic observers. *Vision Research*, *24*, 789–800.

Livingstone, M. S., & Hubel, D. H. (1987). Psychophysical evidence for separate channels for the perception of form, color, movement, and depth. *Journal of Neuroscience*, *7*, 3416–3468.

Mareschal, I., Ashida, H., Bex, P. J., Nishida, S., & Verstraten, F. A. J. (1997). Linking lower and higher stages of motion processing? *Vision Research*, *37*, 1755–1759.

Martinez-Conde, S., Macknik, S. L., & Hubel, D. H. (2000). Microsaccadic eye movements and firing of single cells in the striate cortex of macaque monkeys. *Nature Neuroscience*, *3*, 251–258.

McKee, S. P., & Nakayama, K. (1984). The detection of motion in the peripheral visual field. *Vision Research*, *24*, 25–32.

Murakami, I. (1995). Motion aftereffect after monocular adaptation to filled-in motion at the blind spot. *Vision Research*, *35*, 1041–1045.

Murakami, I., & Cavanagh, P. (1998). A jitter after-effect reveals motion-based stabilization of vision. *Nature*, *395*, 798–801.

Murakami, I., & Cavanagh, P. (1999). A directionally selective monocular adaptation process and a distinctive bilateral compensation process for visual jitter. *Investigative Ophthalmology and Visual Science*, *40*, S2.

Murakami, I., & Cavanagh, P. (2000). Storage, spatial frequency selectivity, and stimulus size specificity of visual jitter. *Investigative Ophthalmology and Visual Science*, *41*, S794.

Murakami, I., & Shimojo, S. (1995). Modulation of motion aftereffect by surround motion and its dependence on stimulus size and eccentricity. *Vision Research*, *35*, 1835–1844.

Murakami, I., & Shimojo, S. (1996). Assimilation-type and contrast-type bias of motion induced by the surround in a random-dot display: evidence for center-surround antagonism. *Vision Research*, *36*, 3629–3639.

Newsome, W. T., Britten, K. H., & Movshon, J. A. (1989). Neuronal correlates of a perceptual decision. *Nature*, *341*, 52–54.

Nishida, S., & Sato, T. (1992). Positive motion after-effect induced by bandpass-filtered random-dot kinematograms. *Vision Research*, *32*, 1635–1646.

Over, R., Broerse, J., Crassini, B., & Lovegrove, W. (1973). Spatial determinants of the aftereffect of seen motion. *Vision Research*, *13*, 1681–1690.

Patti, A. J., Tekalp, A. M., & Sezan, M. I. (1998). A new motion-compensated reduced-order model Kalman filter for space-varying restoration of progressive and interlaced video. *IEEE Transactions on Image Processing*, *7*, 543–554.

Pelz, J. B., & Hayhoe, M. M. (1995). The role of exocentric reference frames in the perception of visual direction. *Vision Research*, *35*, 2267–2275.

Power, R. P. (1983). Apparent movement induced by afterimages. *Perception*, *12*, 463–467.

Raiguel, S., Van Hulle, M. M., Xiao, D.-K., Marcar, V. L., Lagae, L., & Orban, G. A. (1997). Size and shape of receptive fields in the medial superior temporal area (MST) of the macaque. *Neuroreport*, *8*, 2803–2808.

Raiguel, S., Van Hulle, M. M., Xiao, D.-K., Marcar, V. L., & Orban, G. A. (1995). Shape and spatial distribution of receptive fields and antagonistic motion surrounds in the middle temporal area (V5) of the macaque. *European Journal of Neuroscience*, *7*, 2064–2082.

Riggs, L. A., Armington, J. C., & Ratliff, F. (1954). Motions of the retinal image during fixation. *Journal of the Optical Society of America*, *44*, 315–321.

Riggs, L. A., Ratliff, F., Cornsweet, J. C., & Cornsweet, T. N. (1953). The disappearance of steadily fixated visual test objects. *Journal of the Optical Society of America*, *43*, 495–501.

Sereno, M. I., Dale, A. M., Reppas, J. B., Kwong, K. K., Belliveau, J. W., Brady, T. J., Rosen, B. R., & Tootell, R. B. H. (1995). Borders of multiple visual areas in humans revealed by functional magnetic resonance imaging. *Science*, *268*, 889–893.

Shenoy, K. V., Bradley, D. C., & Andersen, R. A. (1999). Influence of gaze rotation on the visual response of primate MSTd neurons. *Journal of Neurophysiology*, *81*, 2764–2786.

Skavenski, A. A., Hansen, R. M., Steinman, R. M., & Winterson, B. J. (1979). Quality of retinal image stabilization during small natural and artificial body rotations in man. *Vision Research*, *19*, 675–683.

Spigel, I. M. (1960). The effects of differential post-exposure illumination on the decay of a movement after-effect. *Journal of Psychology*, *50*, 209–210.

Spigel, I. M. (1962). Contour absence as a critical factor in the inhibition of the decay of a movement aftereffect. *Journal of Psychology*, *54*, 221–228.

Spigel, I. M. (1964). The use of decay inhibition in an examination of central mediation in movement aftereffects. *Journal of General Psychology*, *70*, 241–247.

Steinman, R. M., Haddad, G. M., Skavenski, A. A., & Wyman, D. (1973). Miniature eye movement. *Science*, *181*, 810–819.

Tanaka, K., Hikosaka, K., Saito, H., Yukie, M., Fukada, Y., & Iwai, E. (1986). Analysis of local and wide-field movements in the superior temporal visual areas of the macaque monkey. *Journal of Neuroscience*, *6*, 134–144.

Tanaka, K., Sugita, Y., Moriya, M., & Saito, H. (1993). Analysis of object motion in the ventral part of the medial superior temporal area of the macaque visual cortex. *Journal of Neurophysiology*, *69*, 128–142.

Thompson, P., & Wright, J. (1994). The role of intervening patterns in the storage of the movement aftereffect. *Perception*, *23*, 1233–1240.

Tootell, R. B. H., Reppas, J. B., Kwong, K. K., Malach, R., Born, R. T., Brady, T. J., Rosen, B. R., & Belliveau, J. W. (1995). Functional analysis of human MT and related visual cortical areas using magnetic resonance imaging. *Journal of Neuroscience*, *15*, 3215–3230.

Ts'o, D. Y., Gilbert, C. D., & Wiesel, T. N. (1986). Relationships between horizontal interactions and functional architecture in cat striate cortex as revealed by cross-correlation analysis. *Journal of Neuroscience*, *6*, 1160–1170.

Tulunay-Keesey, U., & VerHoeve, J. N. (1987). The role of eye movements in motion detection. *Vision Research*, *27*, 747–754.

Van Essen, D. C., Newsome, W. T., & Bixby, J. L. (1982). The pattern of interhemispheric connections and its relationship to extrastriate visual areas in the macaque monkey. *Journal of Neuroscience*, *2*, 265–283.

Verstraten, F. A. J., Fredericksen, R. E., Grüsser, O.-J., & van de Grind, W. A. (1994). Recovery from motion adaptation is delayed by successively presented orthogonal motion. *Vision Research*, *34*, 1149–1155.

Verstraten, F. A. J., Fredericksen, R. E., van Wezel, R. J. A., Lankheet, M. J. M., & van de Grind, W. A. (1996). Recovery from adaptation for dynamic and static motion aftereffects: evidence for two mechanisms. *Vision Research*, *36*, 421–424.

Wertheim, A. H. (1987). Retinal and extraretinal information in movement perception: how to invert the Filehne illusion. *Perception*, *16*, 299–308.

Wiesenfelder, H., & Blake, R. (1990). The neural site of binocular rivalry relative to the analysis of motion in the human visual system. *Journal of Neuroscience*, *10*, 3880–3888.

Wiesenfelder, H., & Blake, R. (1992). Binocular rivalry suppression disrupts recovery from motion adaptation. *Visual Neuroscience*, *9*, 143–148.

Wohlgemuth, A. (1911). On the after-effect of seen movement. *British Journal of Psychology*, *1*, 1–117.

Xiao, D.-K., Raiguel, S., Marcar, V., Koenderink, J., & Orban, G. A. (1995). Spatial heterogeneity of inhibitory surrounds in the middle temporal visual area. *Proceedings of the National Academy of Sciences of the USA*, *92*, 11303–11306.

Yarbus, A. L. (1967). *Eye Movements and Vision*. New York: Plenum.